university of groningen / faculty of science and engineering

Bachelor thesis

Relativistic coupled cluster calculations of the ionization potential and electron affinity of Darmstadtium (Z=110)

Author:
E. Mulder

First examinor:
Prof. A. Borschevsky
Second examinor:
Prof. T.L.C Jansen

Faculty of Science and Engineering
University of Groningen
Groningen, the Netherlands

November 25th, 2024

Acknowledgements

First of foremost, I want to thank my first supervisor, Prof. Borschevsky, for helping me get familiar with the subject, for always being available for questions and meetings, and for providing me with valuable feedback throughout the process at any time. I also want to extend my gratitude to Dr. Aucar, for always going out of his way to help me when I ran into an issue with my calculations. His help and kindness were of great value to my research. Furthermore, I would like to thank Prof. Pašteka for his excellent explanation of the CBS limit to me, and for giving valuable tips that were of great help to my calculations. I want to thank Yuly Chamorro Mena for being available for questions and help and for checking in with my progress. I also want to thank my second examinor, Prof. T.L.C Jansen. My gratitude also goes to everyone else in the group and at the Van Swinderen Institute, for making me feel welcome and included. They have made my time researching very enjoyable.

Abstract

Calculations of the ionization potential and electron affinity of darmstadtium were made in a relativistic framework. Various methods and basis sets were used until convergence within meV's was reached. The methods used were DHF, CCSD and CCSD(T), paired with the basis sets from K.G. Dyall. The same methods were used for calculations of the experimentally established ionization potential and electron affinity of the lighter homologue platinum. Relativistic calculations were compared to non-relativistic calculations and the accuracy of the X2C Hamiltonian was compared to that of the 4C Hamiltonian. The final results were obtained with the Dirac Coulomb Hamiltonian, the CCSD(T) method and a complete basis set extrapolation on the d-aug-ae$N$z basis sets. This yielded an IP of 9.748 eV and an EA of 1.034 eV for Ds. The results for Pt suggest that higher order corrections will impose a negative correction within the deV range on the calculated ionization potential and electron affinity values.

Contents

1 Introduction

Thorough knowledge of the atomic-scale properties of periodic elements is essential to understanding the phenomena in our macroscopic world. Traditionally, insight on chemical and physical properties of elements is often gained by analyzing experimental data obtained from spectroscopy experiments on small atoms and molecules. However, moving further down the periodic table to the heavier elements, challenges start to arise concerning the conduction of such experiments.

Transactinides are elements with atomic number $\geq$ 104 and are classified as superheavy elements (SHEs) [1]. They are not naturally found on earth and must be synthesized via nuclear fusion reactions, of which the quantitative yield is often low. Thus far, the heaviest element created in this manner is oganesson (Z=118), while the search for more extensions to the periodic table remains ongoing [2].
What sparks the interest of many scientists is the fact that SHEs often exhibit unexpected properties due to relativistic effects on their electrons [3]. This is caused by the largely increased electron velocities resulting from the strong pull of their highly charged atomic nuclei [4]. Therefore, while SHEs do not have any practical applications as of now, studying their properties can help scientists to better explain certain trends in the periodic table [5]. Moreover, models of atomic structure, nuclear physics and chemical behavior may be refined with the understanding of relativistic effects on atoms and by gaining more insights into the strong nuclear force holding atomic nuclei together. Furthermore, SHEs are of interest to astrophysicists as they are thought to be created in the merging of neutron starts [6]. Understanding their formation and properties can deepen the knowledge of the universe and of nuclear synthesis [2] [7].
While interesting in many ways, most SHEs are very unstable due to the electrostatic repulsion between the large number of protons in their nuclei. This instability leads to a rapid decay within instants for most isotopes, making them unsuitable for experiments. Furthermore, while a few isotopes have been produced with life-times long enough to conduct chemical experiments, it remains a challenge to isolate enough material for such experiments [5]. Therefore, it is of great importance to gain chemical and physical information in a different manner.

In cases where experimental studies are unfeasible, theoretical approaches provide an alternative way to gain information on atomic and molecular properties. These approaches use well-established models, combined with computational methods to accurately estimate certain properties. For chemical problems that involve a detailed understanding of the electronic structure of atoms and molecules, the field of quantum chemistry utilizes the theory of quantum mechanics for computational investigations. Quantum chemistry focuses on applying the Schrödinger equation to accurately calculate the electronic structure and properties of atoms and molecules, while invoking appropriate approximations to the exact theory [8] [9].

In this thesis, calculations are made of the ionization potential (IP) and electron affinity (EA) of the superheavy element darmstadtium (Ds, Z=110) using quantum chemical methods. The methods used are Dirac Hartree Fock (DHF) and coupled cluster method paired with Dyall basis sets. First, calculations of the IP and EA of the lighter homologue of Ds, platinum (Pt, Z=78), are performed of which experimental values are well established. Then, calculations are made on the IP and EA of Ds. The methods are improved gradually until convergence within meVs is reached for the IP and EA.

Calculating the IP and EA of darmstadtium will contribute to the understanding of properties of SHEs and will help compare and understand trends in the periodic table. Furthermore, the results will provide a guideline for possible future spectroscopy experiments on the IP and EA of Ds.

2 Background

2.1 Darmstadtium

Darmstadtium (Ds) is a synthetic superheavy element with atom number 110 and an atomic weight of 281u. It is placed in period seven, group ten in the periodic table of elements as seen in Figure 1. This makes Ds a d-block transactinide [10].

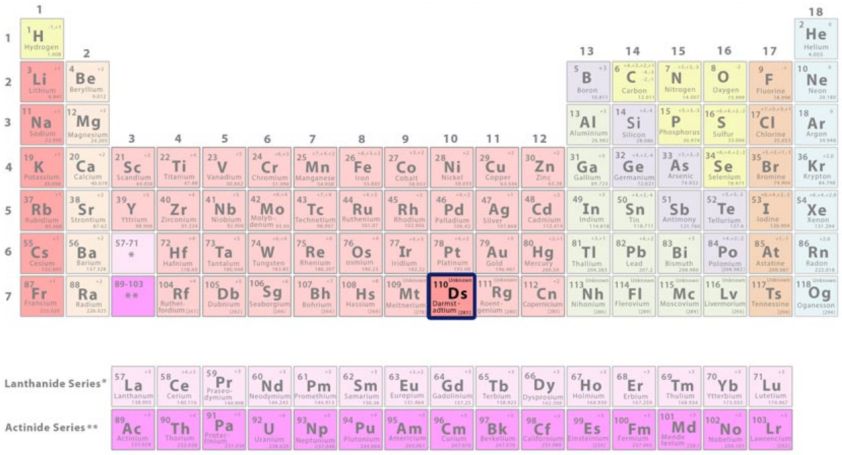

Figure 1: Darmstadtium in the periodic table of elements [11].

Darmstadtium was first synthesised in 1994 in the German city Darmstadt, at the institute for heavy ion research (GSI). It was synthesized via a nuclear fusion reaction in which a ^{208}Pb target was bombarded with accelerated ^{62}Ni nuclei, after which a single ^{269}Ds atom was detected: ${}^{82}_{208}\mathrm{Pb} + {}^{28}_{62}\mathrm{Ni} \rightarrow {}^{110}_{269}\mathrm{Ds} + {}^{1}_{0}\mathrm{n}$. Other isotopes of Ds were subsequently discovered when different isotopes were employed in the fusion reaction, or by observing the products of the decay of heavier elements [12]. The isotopes discovered so far have half-lifes ranging from a few microseconds (^{267}Ds), to fourteen seconds (^{281}Ds) [10]. There are however future prospects for a more stable Ds isotope. Similar to electron shells, atoms have neutron shells that are most stable when filled completely. The amount of neutrons corresponding to a filled configuration are referred to as 'magic numbers'. A magic number for SHEs is N=184. This would correspond to a ^{294}Ds isotope, which is not yet discovered but may be so in the future [13]. For now, the short half-lifes and the small quantities in which the Ds nuclei are produced are the reason that experimental data on the element is scarce. Consequently, its properties have to be predicted with highly accurate calculations.

The electronic ground state configuration of Ds is predicted to be [Rn]$5f^{14}6d^{8}7s^{2}$ [1] [14]. Its valence shells are filled in a different order than those of its lighter homologue platinum (Pt), which is placed in period six, group ten in the periodic table. Platinum (Z=78) has the experimentally confirmed electronic configuration [Xe]$4f^{14}5d^{9}6s^{1}$ [15]. This difference in electronic configuration is a consequence of relativistic effects that become important for heavy elements. Relativistic contraction of the s-orbitals significantly lowers the energy of the valence 7s orbital of Ds, rendering it energetically more favorable for this orbital to be filled first rather than for an electron to be transferred to the d-orbital like in Pt [4]. See section 3.1 for more details on

relativistic effects.
Being in the same group, darmstadtium is expected to have similarities to platinum in spite of their different electronic structures. For Pt, the ionization potential and electron affinity are well established by experiment. These values can be used cautiously as a reference for calculations on Ds, for the consequence of relativistic effects on trends in the periodic table is still under research for SHEs.

2.2 Ionization potential and electron affinity

Ionization potential (IP) and electron affinity (EA) are important characteristics of an atom. They give insight in electronic structure, stability, chemical behavior and periodic trends. Ionization potential is the energy required to remove the outermost electron from a neutral atom. Electron affinity is the opposite: it is the energy gained or required for an electron to be added to a neutral atom. Here, we indicate a positive EA when energy is released in this process, and a negative EA when energy is gained in this process. Both the IP and EA are measured in the gas phase [16].
Generally, IP and EA increase across the periodic table and decrease down the periodic table. Across the periodic table, atomic radii decrease while the nuclear charge increases. Therefore, the outermost electrons feel a stronger pull towards the nucleus, increasing the energy required to remove them. Furthermore, across the periodic table atoms tend to accept additional electrons more easily because this brings them closer to completing their valence shell [17].
Down the periodic table, atomic radii increase due to the higher principle quantum number, while the valence electrons are more shielded from the nuclear charge by the non-valence electrons. This results in the valence electrons experiencing a lower effective nuclear charge, requiring less energy to be removed and making it less favorable to add an extra electron [17]. Figure 2 gives an overview of the trends for the IP and EA within the periodic table.

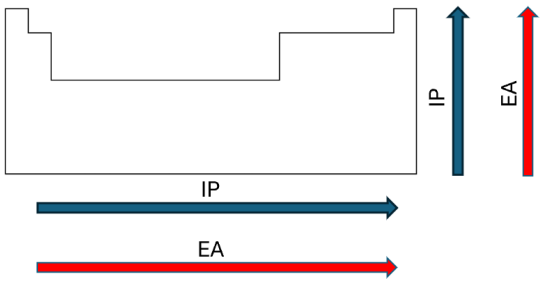

Figure 2: Overview of the general periodic trends for EA and IP.

When forming an ion, Pt has the electron in its 6s orbital removed to obtain the configuration $[Xe]4f^{14}5d^9$ [15]. When forming an anion, an electron is added to the 6s orbital, obtaining the configuration $[Xe]4f^{14}5d^96s^2$ [18]. For Ds, when forming an ion, an electron is removed from the $6d_{5/2}$ orbital to obtain the configuration $[Rn]5f^{14}6d^77s^2$ [1]. When forming an anion, an electron is added to the $6d_{5/2}$ orbital to obtain the configuration $[Rn]5f^{14}6d^97s^2$.
The EA and first IP of Pt are respectively 2.1251 eV [18] and 8.9588 eV [15]. For Ds, there exist no peer-reviewed works about its EA yet. The calculated IP for Ds using density functional

theory is 9.6 eV [1], which is higher then the IP established for Pt. According to Figure 2, the IP of Ds is expected be lower then that of its lighter homologue Pt. This contradiction may be explained by considering relativistic effects on the fine-structure of both atoms.

3 Theory

In this section, the relevant theories and equations to understand the computational methods used are presented. First, the concept of relativity and its effects on the structure of heavy atoms are explained. Then, the two computational methods used in this thesis: Dirac Hartree Fock and coupled cluster method are discussed. After that, the differences between Hamiltonians used in relativistic calculations is shortly elaborated on. Finally, the concept of basis sets is introduced and explained in the context of this thesis.

3.1 Relativity

In classical, non-relativistic physics, the speed of light c is taken to be infinitely large. This is a reasonable estimate when all other particles in a system move relatively slow, and has been the basis of many theoretical models. However, in the real world, the speed of light is finite (c = 299,792,458 m/s [19]) and peculiar things start to occur when particles approach that speed. These effects are called relativistic effects. They come into play for heavy elements and effect their structure and properties.

3.1.1 Atomic structure

As atoms increase in atomic number Z, their positive nuclear charge increases due to the addition of protons. Therefore, the surrounding inner electrons experience a stronger pull towards the nucleus. To prevent the electrons from being pulled in, their speeds have to increase substantially up to a fraction of the speed of light. Einstein's theory of relativity states that the mass m of a moving object with velocity v increases relative to its rest mass m_0 [20]:

$$m = \frac{m_0}{\sqrt{(1 - \frac{v^2}{c^2})}} \tag{1}$$

The relativistic mass correction inversely scales with the orbital angular momentum l. It is especially pronounced for s-orbitals with $l = 0$, but also for p-orbitals with $l = 1$. Their probability densities are high around the nucleus, whereas higher l-orbitals have more angular nodes in their wavefunction for which they seldom spend time near the nucleus. The increased electron mass in turn results in the relative contraction of the s- and $p_{1/2}$-orbitals. The radial distance of the orbitals is given by [21]:

$$r = \frac{Ze^2}{4\pi\epsilon_0 m v^2} \tag{2}$$

in which e is the elementary charge and ϵ_0 is the vacuum permittivity. This distance decreases for the increased mass of the inner electrons. This contraction, called the direct relativistic effect, is observed for all s- and $p_{1/2}$-orbitals up to the valence shell. This is because their electron speeds increase comparably in the vicinity of the nucleus, contracting the inner parts of the wavefunction which in turn pull in the outer tail. Consequently, these contracted s- and p-orbitals effectively shield the electrons in the d- and f-shells from the nuclear charge. Therefore, they experience a weaker attraction towards the nucleus and as a consequence expand radially. This orbital expansion of the higher valued l shells is called the indirect relativistic effect [4] [21].

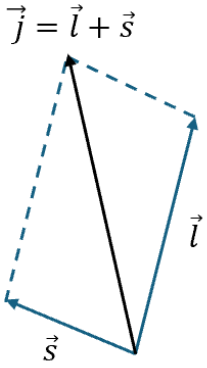

Figure 3: The total angular momentum vector $\vec{j}$ as the vector sum of the orbital angular momentum vector $\vec{l}$ and the spin angular momentum vector $\vec{s}$.

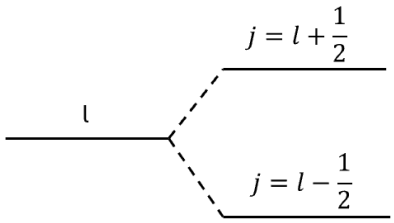

Figure 4: The energetic fine-splitting of an orbital with $l > 0$.

Another relativistic effect impacting the fine-structure of heavy atoms is spin-orbit coupling. The relative motion of the positively charged nucleus with respect to the negatively charged orbiting electrons induces a magnetic field, which exerts a torque on the spin angular momentum vector $\vec{s}$. This causes the orbital angular momentum vector $\vec{l}$ and the spin angular momentum vector to precess about each other. This interaction is called the spin-orbit interaction. It is described by the vector sum of the angular momenta [22]:

$$\vec{j} = \vec{l} + \vec{s} \tag{3}$$

in which $\vec{j}$ is the total angular momentum vector, as depicted in Figure 3. j is a quantum number that can take on the values $|l \pm \frac{1}{2}|$, since $s = \frac{1}{2}$ for electrons. An orbital angular momentum quantum number is specified with its j-value using the following notation: l_j. The energetic splitting between these j-levels for l-values higher than zero is a third relativistic effect, depicted in Figure 4. The magnitude of this effect increases with atomic size [4] [22].

3.2 (Dirac) Hartree Fock method

The following section is based on references [23], [24] and [25].

The Hartree Fock (HF) method is the fundament for computations of the electronic configuration of atoms and molecules. It is an 'ab initio' method that requires no empirical input: it uses an appropriate Hamiltonian for the system and a model form of its electronic wave function to calculate the ground state energy of the system. HF is build on the variation principle, which states that the calculated energy of the system is always equal to or higher than the exact energy. HF therefore operates by iteratively optimizing the initial guess of molecular orbitals in order to minimize the calculated energy, until a set convergence criterion is met.

Each electron in an atom can be described by its spatial orbital $\phi(\mathbf{r})$ and by its spin state

$\omega = \{\alpha, \beta\}$. To describe both spatial and spin states simultaneously, the spin orbital $\chi(\mathbf{x})$ is introduced, in which $\mathbf{x} = \{\mathbf{r}, \omega\}$. To simplify the situation, the independent particle model is used as an approximation. This implies that there are no direct electron-electron interactions; each electron experiences an average potential of the nucleus and all other electrons. In this way, the total spin wave function describing N electrons can be written as the product of each individual spin orbital, called the Hartree Product:

$$\Psi_{HP}(\mathbf{x}_1, \mathbf{x}_2, ..., \mathbf{x}_N) = \chi_1(\mathbf{x}_1)\chi_2(\mathbf{x}_2)...\chi_N(\mathbf{x}_N) \tag{4}$$

For fermions, however, an important criterion to the total wave function is that it must be anti-symmetric under exchange of two particles. For two electrons, this principle is satisfied by the following form:

$$\Psi(\mathbf{x}_1, \mathbf{x}_2) = \frac{1}{\sqrt{2}}[\chi_1(\mathbf{x}_1)\chi_2(\mathbf{x}_2) - \chi_1(\mathbf{x}_2)\chi_2(\mathbf{x}_1)] \tag{5}$$

Or, in determinant notation:

$$\Psi(\mathbf{x}_1, \mathbf{x}_2) = \frac{1}{\sqrt{2}} \begin{vmatrix} \chi_1(\mathbf{x}_1) & \chi_2(\mathbf{x}_1) \\ \chi_1(\mathbf{x}_2) & \chi_2(\mathbf{x}_2) \end{vmatrix} \tag{6}$$

Using the latter notation, this form can be extended to N electrons to make the Hartree Product anti-symmetric:

$$\Psi(\mathbf{x}_1, \mathbf{x}_2, ..., \mathbf{x}_N) = \frac{1}{\sqrt{N}} \begin{vmatrix} \chi_1(\mathbf{x}_1) & \chi_2(\mathbf{x}_1) & ... & \chi_N(\mathbf{x}_1) \\ \chi_1(\mathbf{x}_2) & \chi_2(\mathbf{x}_2) & ... & \chi_N(\mathbf{x}_2) \\ \vdots & \vdots & \ddots & \vdots \\ \chi_1(\mathbf{x}_N) & \chi_2(\mathbf{x}_N) & ... & \chi_N(\mathbf{x}_N) \end{vmatrix} \tag{7}$$

The above notation of a determinant of spin orbitals is called a Slater determinant, and it can be concisely written in bra-ket notation as $|ij...k\rangle$ where each indice is an occupied orbital.

HF was developed to solve the electronic Schrödinger equation:

$$\mathbf{H}\Psi(\mathbf{r},\ \mathbf{R}) = E_{el}\Psi(\mathbf{r},\ \mathbf{R}) \tag{8}$$

In which $\mathbf{H}$ is the Hamiltonian of the system, E_{el} the electronic ground state energy of the system and Ψ the single electronic wave function with $\mathbf{r}$ the radial vector and $\mathbf{R}$ the nuclear coordinates. This equation invokes the Born-Oppenheimer (BO) approximation, which assumes that the wave functions of atomic nuclei and electrons can be treated separately considering the large difference between their masses. The BO approximation considers the atomic nuclei to be fixed in a set of coordinates, while the electrons are dynamic. For an atom, the complete Hamiltonian within the BO approximation is:

$$\mathbf{H} = -\frac{1}{2}\sum_i \nabla_i^2 - \sum_{A,i} \frac{Z_A}{r_{A,i}} + \sum_{i>j} \frac{1}{r_{ij}} \tag{9}$$

Here, the first term corresponds to the kinetic energy, the second term to the nuclear attraction between electrons and nuclei and the final term to the electron repulsion. Equation 9 can be split in terms of two single electron components and a two electron component. This allows for the definition of two operators:

$1e^-$ operator:

$$h(i) = -\frac{1}{2}\nabla_i^2 - \sum_A \frac{Z_A}{r_{i,A}} \tag{10}$$

$2e^-$ operator:

$$g(i,j) = \frac{1}{r_{ij}} \tag{11}$$

Such that the Hamiltonian can be concisely written as:

$$\mathbf{H} = \sum_i h(i) + \sum_{i<j} g(i,j) \tag{12}$$

Rewriting the electronic Schrödinger Equation 8 in bra-ket notation to solve for the energy eigenstates we obtain:

$$E_{el} = \langle \Psi | \mathbf{H} | \Psi \rangle \tag{13}$$

In which we can substitute Equation 12 and the Slater determinant in Equation 7 as the wave function, to arrive at the following expression for the Hartree Fock energy:

$$E_{HF} = \sum_i \langle i|h|i\rangle + \frac{1}{2}\sum_{ij}[(ii|jj) - (ij|ji)] \tag{14}$$

This energy is then minimized computationally in agreement with the variation principle, by iteratively optimizing the initial guess of spin orbitals. HF does so via the method of Lagrange multipliers, which is a method to find the local minimum of a function subject to a constraint. In this case, the constraint is the orthonormality of the spin orbitals. When the difference between the newly calculated energy and the previously calculated energy is smaller then the set convergence criterion, convergence is reached and the calculation is finished.

In a relativistic framework, instead of the classical one-electron operator in Equation 10, the one-electron Dirac operator is used [26]:

$$h_d(i) = c\boldsymbol{\alpha}_i \cdot \mathbf{p} + c^2\beta + V_{nuc} \tag{15}$$

Where $\mathbf{p}$ is the momentum operator, V_{nuc} is the nuclear attraction operator and

$$\boldsymbol{\alpha}_i = \begin{bmatrix} 0 & \sigma_i \\ \sigma_i & 0 \end{bmatrix}, \beta = \begin{bmatrix} I_2 & 0 \\ 0 & -I_2 \end{bmatrix}$$

where σ_i are the Pauli spin matrices and I_2 is the 2×2 identity matrix [27]. The Hamiltonian in Equation 12 can then be written as

$$\mathbf{H}_{DC} = \sum_i h_d(i) + \sum_{i<j} g(i,j) \tag{16}$$

which is named the Dirac Coulomb Hamiltonian [28].

The calculated Hartree Fock energy does not account for electron-electron interactions, making it only a rough estimate of the exact ground state energy. Therefore, post Hartree Fock methods are intended to calculate the correlation energy, which is the difference between the exact ground state energy and the Hartee Fock energy [25]:

$$E_c = E_0 - E_{HF} \tag{17}$$

3.3 Coupled cluster method

Coupled cluster method is a post-Hartree Fock method that corrects the Hartree Fock wave function by including the previously ignored effects of electron correlation. The wave function is now decomposed in terms of the excitation cluster amplitudes of a finite number of electrons [29]. This corrected wave function is then used to calculate the correlation energy of the system, which is added to the Hartree Fock energy to obtain the coupled cluster ground state energy of the system.

Within the HF method, the wave function was composed of a Slater determinant of the one-electron wave functions describing the occupied states of the system. These occupied states are referred to as the Fermi sea [29]. Correlation between a cluster of electrons is described by an interaction in which they lift themselves out of the Fermi sea to an excited state, as depicted in figure 5a for two electrons. This interaction can happen between m electrons and the resulting wave function can be described by an operator $\hat{T}_m$ acting on the original HF wave function: $\hat{T}_m|\Psi_{HF}\rangle$ [30] where

$$\hat{T}_m = \sum_{\substack{i>j>\ldots m \\ a>b>\ldots m}} t_{ij\ldots}^{ab\cdots} \hat{a}_a^\dagger \hat{a}_b^\dagger \cdots \hat{a}_j \hat{a}_i, \tag{18}$$

[31]. Here, $t_{ij\ldots}^{ab\cdots}$ are the to be determined excitation cluster amplitudes, $\hat{a}_a^\dagger$ is the creation operator for the virtual orbital a and $\hat{a}_i$ is the annihilation operator for the occupied orbital i [25].
Multiple clusters of m electrons can also be excited simultaneously n times, as depicted in Figure 5b for a double excitation of a two electron cluster. This process is described by applying $\hat{T}_m$ n times while including a statistical weighing of $\frac{1}{n!}$ to avoid counting clusters twice [29]. The total amplitude of the correlation of an arbitrary number n independent clusters with each m electrons is then:

$$\sum_{n=0} \frac{1}{n!} \hat{T}_m |\Psi_{HF}\rangle = e^{\hat{T}_m} |\Psi_{HF}\rangle$$

Clusters of different sizes can also be simultaneously excited. Using linear superposition and summing over all possibilities, the amplitude for the simultaneous excitation of n singles ($\hat{T}_1$) and k doubles ($\hat{T}_2$) is [29]:

$$\sum_{n,k} \frac{1}{n!k!} \hat{T}_1^n \hat{T}_2^k = e^{(\hat{T}_1 + \hat{T}_2)}$$

Proceeding in this manner up to a cluster of N electrons, we arrive at the wave function [25]

$$e^{(\hat{T}_1 + \hat{T}_2 + \hat{T}_3 + \ldots \hat{T}_N)} |\Psi_{HF}\rangle = e^{\hat{T}} |\Psi_{HF}\rangle \tag{19}$$

where $\hat{T}$ is the total cluster operator [29]. This wave function describes the total electronic wave function including all possible electron correlations up to a cluster of N electrons, and is called the coupled cluster wave function [25]:

$$|\Psi_{CC}\rangle = e^{\hat{T}} |\Psi_{HF}\rangle \tag{20}$$

The cluster operator is often truncated up to a certain term to ease calculations for larger systems. This approximation can be justified by the fact that for a many-electron system, the surrounding neighbours of an electron effectively shield it from other electrons. Therefore, the electron interacts with relatively few other particles [29] [32].

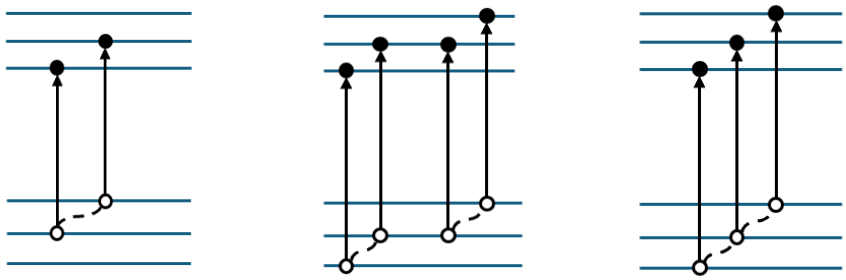

(a) A single excitation of a two-electron cluster: n=1, m=2.

(b) A double excitation of two two-electron clusters: n=2, m=2.

(c) A single excitation of a three-electron cluster: n=1, m=3.

Figure 5: Three examples of electrons correlating with each other and lifting themselves out of the Fermi sea.

3.3.1 CCSD

A widely used method for relatively small calculations is the coupled cluster singles doubles (CCSD) method, in which the cluster operator is truncated such that only the terms for single and double electron excitations remain: $\hat{T} = \hat{T}_1 + \hat{T}_2$. The CCSD wave function is given by [25]:

$$|\Psi_{CCSD}\rangle = e^{(\hat{T}_1+\hat{T}_2)}|\Psi_{HF}\rangle \tag{21}$$

with

$$\hat{T}_1 = \sum_{i,a} t_i^a \hat{a}_a^\dagger \hat{a}_i \tag{22}$$

and

$$\hat{T}_2 = \sum_{ij,ab} t_{ij}^{ab} \hat{a}_a^\dagger \hat{a}_b^\dagger \hat{a}_j \hat{a}_i \tag{23}$$

3.3.2 CCSD(T)

Building upon CCSD is the CCSD(T) method, which adds a non-iterative estimate of the excitation of triples. This is achieved by loosely using perturbation theory, in which the converged singles and doubles wave functions from CCSD are used in an energy correction formula. It is computationally much cheaper then fully including triples (CCSDT) but gives the most accurate approximation to CCSDT, which explains its wide usage and popularity among quantum chemists [33] [34].

3.3.3 Energy and amplitude calculation

For the calculation of the coupled cluster ground state energy, the coupled cluster wave function is required to satisfy the Schrödinger Equation 13:

$$(\hat{H} - E)|\Psi_{CC}\rangle = 0 \tag{24}$$

This requirement is then projected onto the sufficient number of excitations corresponding to the truncation level of the cluster operator [31] [25]:

$$\langle \Phi_0 | (\hat{H} - E) | \Psi_{CC} \rangle = 0 \tag{25}$$

$$\langle \Phi_i^a | (\hat{H} - E) | \Psi_{CC} \rangle = 0 \tag{26}$$

$$\langle \Phi_{ij}^{ab} | (\hat{H} - E) | \Psi_{CC} \rangle = 0 \tag{27}$$

continuing downwards for all excited states. When implying Equation 24, the coupled cluster total energy can be given by:

$$E_{CC} = \langle \Phi_0 | \hat{H} | \Psi_{CC} \rangle \tag{28}$$

The rest of the equations (Equation 25 and downward) form a system of non-linear equations that can be solved iteratively for the excitation cluster amplitudes $t_{ij\ldots}^{ab\cdots}$ [25].

3.4 Hamiltonians

The following section is based on references [35] and [36].

Apart from the choice of the computational method used in a theoretical calculation, the choice of Hamiltonian is a second parameter that influences the accuracy of the method.
The one-electron Hamiltonian comes in different dimensions. For non-relativistic calculations, a one-dimensional scalar operator was introduced in Equation 10. Whereas for relativistic calculations, the one-electron Dirac operator in Equation 15 is a 4×4 matrix operator. The Dirac Coulomb Hamiltonian is therefore called a four component (4C) Hamiltonian and it must act on a four component wavefunction. This 4C wavefunction is called a bispinor and is made up of a large component and a small component, both having two components (up and down) for the particle's spin state:

$$\Psi = \begin{bmatrix} \uparrow \\ \downarrow \\ \uparrow \\ \downarrow \end{bmatrix} = \begin{bmatrix} \psi^L \\ \psi^S \end{bmatrix} \tag{29}$$

The large components are associated with positive energy solutions, while the small components are associated with negative energy solutions. In the non-relativistic limit, the small components vanish since they capture relativistic effects such as spin-orbit coupling. The large components carry most of the particle's probability density.

Using a 4C Hamiltonian is computationally quite demanding. To ease calculations, a two-component relativistic Hamiltonian can be generated by the decoupling of the large and small components. The Hamiltoninan is then re-formulated in terms of the large components only, while the relativistic corrections of the small components are still incorporated implicitly. The 4C wave function is decoupled as well, to yield a 2C wave function described in terms of the large components only. The decoupling can be done exactly, yielding the exact two-component relativistic (X2C) Hamiltonian, or approximately. In this thesis, we focus on the X2C Hamiltonian. The exact coupling between the large and small components is given by

$$\psi^S = R\psi^L \tag{30}$$

In which the coupling constant R is given by:

$$R = \frac{c(\sigma \cdot \mathbf{p})}{2mc^2 - V_{nuc} + E^+} \tag{31}$$

Here, σ are the Pauli spin matrices, $\mathbf{p}$ is the momentum operator, V_{nuc} the nuclear potential energy and E^+ the positive-energy solutions. After some manipulation, the positive-energy two-component wave function is obtained:

$$\Psi_+^{2C} = \sqrt{1 + R^\dagger R}\, \psi^L \tag{32}$$

On which the 2C Hamiltonian will act. The X2C Hamiltonian is given by:

$$h_+ = \sqrt{1 + R^\dagger R}\, [h_{11} + h_{12} R] \frac{1}{\sqrt{1 + R^\dagger R}} \tag{33}$$

In which h_{11} is the part of the parent Hamiltonian that couples between the large-large components and h_{12} is the part that couples between the large and small components. The X2C Hamiltonian reproduces the positive energy spectrum of the 4C Hamiltonian while incorporating the effects of the small components implicitly.

In the previous methods and Hamiltonians, electrons were considered static with an average interaction between each other. The Breit correction is an additional term that can be added to the two-electron part of the Dirac Coulomb Hamiltonian, to account for the electromagnetic interactions between electrons and for retardation effects that result from the finite speed of light [37]. Further corrections account for quantum electrodynamics (QED), which describes the interactions between charged particles in the form of photon exchange. This correction is implemented in the model Lamb shift operator, which accounts for vacuum polarization, electron self-energy, cross terms and higher order QED effects [26] [38].

3.5 Basis sets

3.5.1 Gaussian type orbitals

For theoretical calculations on the electronic structure of an atom or molecule, their electronic wave function needs to be mathematically modeled. The set of functions used in such a model is called a basis set. Alongside the choices of computational method and Hamiltonian used, the choice of basis set provides a third parameter able to specify the accuracy of a calculation. A basis set mathematically approximates the orbitals of an atom, by using a linear combination of functions to describe the orbitals. Basis sets come in different sizes and properties, varying in accuracy and computational cost. The larger a basis set is, the less restrictions it imposes on the location of the electrons. Consequently this yields a more accurate description of the orbitals, but costs a higher computational price [39] [40].

For electronic structure calculations, the universally used functions are Gaussian type orbitals (GTOs). In Cartesian coordinates, they have the following form:

$$g_{ijk} = N x^i y^j z^k e^{-\alpha r^2} \tag{34}$$

where N is a normalization constant, i, j and k sum up to the orbital angular momentum l of the atomic orbital, x, y, z define the Cartesian distance between the electron and the GTO and α is an exponent that defines the radial distance of the orbital function [40]. The form of Equation 34 is called a primitive function. To use more functions while keeping computational costs low, primitive functions are often linearly combined to obtain what is called a contracted function. Basis sets thus contain contracted functions to describe the atomic orbitals, which are each made up of primitive Gaussian functions [39].

A minimal basis sets contains the minimal amount of Gaussian functions to describe the orbitals of an atom. It only describes the non-virtual, occupied orbitals. For example, for carbon which has six electrons with configuration $1s^2 2s^2 2p^2$, a minimal basis set would consist of a description of the $1s, 2s, 2p_x, 2p_y, 2p_z$ orbitals.
A basis set can be expanded by taking more then one basis function per valence orbital. These basis functions describing the same orbital differ in size. The notation used for this is nz, where n corresponds to the amount of basis functions used for each orbital. For the previous example of carbon, a double-zeta (2z) basis set would contain $1s, 2s, 2s', 2p_x, 2p_y, 2p_z, 2p'_x, 2p'_y, 2p'_z$ orbitals. This type of basis set is called a split-valence basis set.
Besides adding extra valence orbitals, a basis set can also be expanded by the addition of polarization functions, which describe virtual orbitals with angular momenta that are beyond the ground state description of an atom. For carbon, this would be the addition of a d-orbital.
Finally, diffuse functions can be added to a basis set, which are characterized by their small exponents. These functions occupy a larger volume in space and thereby provide a description of the region far from the nucleus [39].

3.5.2 Dyall basis sets

There exist several families of basis sets differing in composition, such as the Dunning or Pople basis sets [40]. In this thesis, the Dyall basis sets designed by K. G. Dyall are employed. These basis sets are optimized for relativistic calculations and consist of uncontracted Gaussian functions.
The minimal basis sets employed are the vNz split-valence sets, where N is the basis set cardinality ($N = 2, 3, 4.$). For d-block atoms such as Pt and Ds, a vNz set inlcudes functions for correlation of the ns, np, nd, and $(n+1)$s orbitals. Another type of basis sets are the core-valence sets cv$N$z, which additionally include functions for the correlation of lower-lying (n-1) shells. Finally, the all-electron basis sets ae$N$z are basis sets that correlate all electrons in a system.
Each of the previously mentioned basis set may be augmented by the addition of a single, double or triple diffuse function to each symmetry. An augmented basis set is denoted by the prefix x-aug- (x = s, d, t, ..) [41].

3.5.3 Complete basis set limit

Using large basis sets is a trade-off between accuracy and computational cost. Ideally, a complete basis set (CBS) would be used. A complete basis set would be infinitely large, with its calculation results converging to the exact solution of the Schrödinger equation. Since this is computationally out of reach, extrapolation schemes can be used to reproduce the CBS limit using the results of finite basis set calculations. These schemes are based on the asymptotic convergence of energies resulting from systematic effects of basis sets. The extrapolations are done with energy results of

the same basis set but with increasing cardinality. For the DHF energy, the following three-point extrapolation scheme is employed [42]:

$$E_{CBS}^{DHF} = \frac{E(2z)E(4z) - E(3z)^2}{E(2z) - 2E(3z) + E(4z)} \tag{35}$$

whereas for the correlation energy from coupled cluster calculations, the two-point extrapolation scheme for triple and quadrupole cardinality:

$$E_{CBS}^{corr} = \frac{27E(3z) - 64E(4z)}{-37} \tag{36}$$

is used [42]. The correlation energy can be added to the DHF energy to yield the total CBS energy [42].

$$E_{CBS}^{Tot} = E_{CBS}^{DHF} + E_{CBS}^{corr} \tag{37}$$

4 Results

All calculations were performed using the DIRAC23 program [43] on the Hábrók HPC cluster [44], using the MobaXterm application [45]. Energies were originally given in atomic units (a.u.) and then converted to electron volts (1 a.u. = 27.211 386 245 981 eV [46]).

4.1 Platinum

In this section, the computational results for Platinum are presented. The experimental IP and EA of Pt are 8.9588 eV [15] and 2.1251 eV [18] respectively. It is not necessarily expected that the best calculation will give the best agreement with experiment, as these results lack higher order corrections such as the Breit and QED corrections and higher order excitations. Convergence of the results within meV's with respect to increasing the method is searched after.

Considering relativistic j-splitting, the fully occupied $5d_{3/2}$ shell is treated as a closed shell and the partially occupied $5d_{5/2}$ shell is treated as an open shell. Results did not converge when specifying two open shells; one with 1 electron in two active spinors ($6s^1$) and the other with 5 electrons in 6 active spinors ($5d^5_{5/2}$). Therefore, the 6 open-shell electrons were specified collectively as being in one open shell with 8 active spinors.
For the coupled cluster calculations, the orbitals with energies between -30 a.u. and +30 a.u were used for vnz and cvnz calculations. For the aenz basis sets, the orbital with energies between -3000 a.u. and +2000 a.u. were used and all electrons were correlated.

Table 1: The calculated IPs and EAs of Pt in eV using DHF, CCSD and CCSD(T) with different Dyall basis sets.

	IP			EA		
	DHF	CCSD	CCDS(T)	DHF	CCSD	CCSD(T)
v2z	6.8653	8.7323	8.8169	-0.0263	1.4638	1.7539
v3z	6.8747	8.8767	8.9804	0.3570	1.5882	1.2522
cv3z	6.8747	8.8972	9.0195	0.3571	2.0886	1.7763
ae3z	6.8747	8.8949	9.0314	0.3571	1.7565	2.0692
s-aug-v3z	6.8760	8.8844	8.9896	0.4699	1.5060	1.1594
v4z	6.8730	8.9168	9.0177	0.4385	1.7949	2.1545
cv4z	6.8730	8.9294	9.0483	0.4385	1.8055	2.1504
ae4z	6.8730	8.9241	9.0326	0.4385	1.8305	2.1761
s-aug-v4z	6.8732	8.9180	9.0141	0.4698	1.8172	2.1878
d-aug-v4z	6.8732	8.9181	9.0145	0.4703	1.8175	2.1874
t-aug-v4z	6.8732	8.9190	9.0151	0.4703	1.8176	2.1867
s-aug-cv4z	6.8732	8.9313	9.0507	0.4698	1.8280	2.1784
d-aug-cv4z	6.8732	8.9313	9.0509	0.4703	1.8282	2.1781
t-aug-cv4z	6.8732	8.9313	9.0510	0.4703	1.8283	2.1779
s-aug-ae4z	6.8732	8.9287	9.0473	0.4698	1.8512	2.1915
d-aug-ae4z	6.8732	8.9274	9.0461	0.4703	1.8512	2.1915
d-aug-ae$N$z	6.8729	8.9408	**9.0442**	-	-	-

Table 1 summarizes all results from the calculations of Pt, for which the effect of using DHF, CCSD and CCSD(T) with the same basis set can be compared. For the IP of Pt, a clear trend is

observed with regards to increasing the accuracy of the computational method. For every basis set, the IP increases with about 2.0 eV when increasing from DHF to CCSD. When including treatment of perturbative triples, the IP increases again with about an additional 0.1 eV for all basis sets.
For the EA, increasing from DHF to CCSD again results in an increase varying between 1.0-1.7 eV for triple cardinality, and a more constant 1.35 eV for quadrupole cardinality. Again, including treatment of perturbative triples further increases the EA for quadrupole cardinality between 0.34-0.38 eV. For triple cardinality, the contribution of moving from CCSD to CCSD(T) varies between being positive and negative, contributing about +0.3 eV for ae3z and -0.3 eV for v3z, cv3z and s-aug-v3z.
Overall, the IP and EA increase when the level of computational method increases. The biggest increment is observed between DHF and CCSD, demonstrating the large effect of including electron correlation treatment. This effect is the most pronounced for the IP, whereas the inclusion of perturbative triples is the most pronounced for the EA. Furthermore, for quadrupole cardinality the results show clear trends, whereas for triple cardinality, only clear trends are observed for the IP. For the EA, the results with triple cardinality deviate and behave unexpectedly, indicating some linear dependency within the triple zeta calculations involving the Pt anion.

Focusing on CCSD(T) results, the effects of basis sets will be evaluated.

Table 2: CCSD(T) results for split valence basis sets with increasing cardinalities.

CCSD(T)	IP	EA
v2z	8.8169	1.7539
v3z	8.9804	1.2522
v4z	9.0177	2.1545

With Table 2, the effect of increasing the cardinality of a basis set on the IP and EA of Pt can be assessed. For the IP, increasing cardinality from v2z to v3z imposes an increase of 0.16 eV. Further increasing cardinality from v3z to v4z increases the IP with 0.04 eV. For the EA, a clear trend is not observed since increasing cardinality from v2z to v3z decreases the EA with 0.50 eV, whereas increasing cardinality from v3z to v4z increases the EA with 0.90 eV. When assuming a linear dependency within the triple zeta calculations for the EA and thus disregarding these results, the EA does increase when increasing cardinality. The effect of increasing cardinality of a basis set has a larger effect on the EA then on the IP for Pt.

Table 3: CCSD(T) results for the v4z basis set with outer-core correlating functions and inner-core correlating functions.

CCSD(T)	IP	EA
v4z	9.0177	2.1545
cv4z	9.0483	2.1504
ae4z	9.0326	2.1761

With Table 3, the effect of the addition of outer-core correlating functions and inner-core correlating functions to the v4z split-valence basis set can be assessed for the IP and EA of Pt. These effects are of an order smaller then the effects of cardinality, and clear trends cannot be observed. Addition of outer-core correlating functions increases the IP with 31 meV, whereas

the EA decreases with 4 meV. Addition of inner-core correlating functions decreases the IP with 16 meV whereas it increases the EA with 26 meV. The IP is observed to be more sensitive to outer-core correlated functions, whereas the EA is observed to be more sensitive to inner-core correlated functions. Overall, the IP and EA both increase with respect to the split valence basis set when correlating all electrons.

Table 4: CCSD(T) results for the cv4z basis set with the addition of single, double and triple diffuse functions.

CCSD(T)	IP	EA
cv4z	9.0483	2.1504
s-aug-cv4z	9.0507	2.1784
d-aug-cv4z	9.0509	2.1781
t-aug-cv4z	9.0510	2.1779

With Table 4, the addition of diffuse functions can be assessed for the IP and EA of Pt. The effect of the addition of a single layer of diffuse functions is the most notable, and is observed to be of an order larger for the EA (+28 meV) versus for the IP (-2.4 meV). This can be explained by the fact that diffuse functions contribute to the description of the outer part of the of the wave function away from the nucleus, which is important for the loosely bound extra electron that the EA is associated with. The effects of additional layers of diffuse functions are much smaller, and result in the IP being increased with meV's and the EA being decreased with meV's. The results converge with respect to the third digit for the second layer of diffuse functions.

Since the effects on the IP and EA associated with the addition of diffuse functions are mostly independent of cardinality, inner and outer core correlating functions, the results converging for the second layer of diffuse functions in Table 4 implies that the CBS limit can be taken for the d-aug-ae$N$z basis sets. This yielded the final rounded IP of 9.044 eV, where the CBS limit induced a correction of -1.9 meV with respect to the d-aug-ae4z basis set. The EA could not be obtained within the CBS limit, as this would involve the results from the unreliable triple zeta basis set. Therefore, the final result for the EA is obtained with the d-aug-ae4z basis set, yielding a value of 2.192 eV.
The error associated with taking the CBS limit is calculated according to the procedure of [47], for which half of the difference between the CBS result and the d-aug-ae4z result is taken. This yields an error of 0.95 meV for the IP.

Table 5: A comparison of the results obtained with the v4z basis set in a non-relativistic framework; with the exact two-component Hamiltonian and with the Dirac four component Hamiltonian.

	IP			EA		
	DHF	CCSD	CCSD(T)	DHF	CCSD	CCSD(T)
Non-relativistic (c=10000)	11.8704	6.9056	7.1476	3.0584	0.8760	1.1589
Relativistic X2C	6.8479	8.9120	9.0069	0.4487	1.7791	2.1423
Relativistic 4C	6.8730	8.9168	9.0177	0.4385	1.7949	2.1545

In Table 5, the IP and EA obtained with a non-relativistic calculation are compared to those obtained with relativistic calculations, both using the v4z basis set. For the non-relativistic

calculations, in the specification of the electronic configurations for the neutral, positive and negative atom, the valence s- and d-orbitals were treated together as being open. This resulted in the electrons being 'spread out' equally over the orbitals, with 1/6th of the density on the 6s orbital and 5/6th of the density on the 5d orbitals.

With the CCSD and CCSD(T) methods, both the IP and EA are lower in the non-relativistic framework. This can be explained by the difference in electron configurations. In the relativistic frame, an electron is removed from or added to the relativistically contracted and stabilized 6s orbital. The relativistic contraction of this orbital causes its electron to be more tightly bound to the nucleus; increasing the energy threshold to remove it. Furthermore, the EA is raised since the contracted 6s orbital experiences a higher effective nuclear charge; making it energetically favorable for a negatively charged electron to be added. Whereas in the non-relativistic frame, an electron is partially added to or removed from both the 5d and 6s orbitals, which are not contracted or stabilized and thus result in a lower IP and EA. It is unclear why the IP and EA do not follow the above reasoning with DHF calculations, but the large differences between the results obtained with non-relativistic and relativistic calculations highlight the magnitude of treating relativity in heavy atom calculations.

Table 5 also compares the IP and EA obtained with the Dirac 4C Hamiltonian with the IP and EA obtained with the less computationally demanding X2C Hamiltonian. Following the same reasoning as for the non-relativistic calculations, the results are as expected considering that the X2C Hamiltonian incorporates relativistic corrections implicitly. Therefore it is expected that the X2C results are close to the 4C results, but that its values lie between the values of non-relativistic and fully relativistic calculations. This is the case except for the DHF result of the IP.

In terms of accuracy, although X2C calculations provide a good approximation to the fully relativistic 4C results, they are not accurate within meV's. This highlights the importance of using the 4C Hamiltonian when meV's is the accuracy aimed for.

4.2 Darmstadtium

In this section, the computational results for Darmstadtium are shown. Considering relativistic j-splitting, the fully occupied $6d_{3/2}$ shell is treated as a closed shell and the partially occupied $6d_{5/2}$ shell is treated as an open shell. For split-valence and core-valence basis sets, the orbitals with energies between -30 a.u. and +30 a.u. were correlated. For all-electron basis sets, orbitals with energies between -7000.0 and +2000.0 a.u. were correlated such that all occupied orbitals were included.

First, the electronic configuration of Ds is assessed to check whether the closed shell configuration ([Rn] $5f^{14}6d^{8}7s^{2}$) is indeed the configuration with the lowest energy compared to the open shell configuration ([Rn] $5f^{14}6d^{9}7s^{1}$) which is similar to the electronic configuration of Pt. This comparison is done with the s-aug-v4z basis set and the results are shown in Table 6.
The closed shell electronic configuration is indeed lower in energy then the open shell configuration. This is as expected, because strong relativistic effects result in a contraction and stabilization of the 7s orbital, whereas the $6d_{5/2}$ orbital is radially expanded and energetically destabilized. It is therefore energetically more favorable for an electron to be in the 7s orbital then in the $6d_{5/2}$ orbital. The closed shell configuration will therefore be used for the rest of the

Table 6: Comparison of the open shell and closed shell energies for Ds, using the s-aug-v4z basis set.

	open shell energy (a.u.)	closed shell energy (a.u.)	difference (eV)
DHF	-45057.622818727308	-45057.681555201343	-1.5983
CCSD	-45059.157101362543472	-45059.159236354353197	-0.0581
CCSD(T)	-45059.200965249874571	-45059.201645630702842	-0.0185

calculations.

Table 7: The calculated IPs and EAs of Ds in eV using DHF, CCSD and CCSD(T) with different Dyall basis sets.

	IP			EA		
	DHF	CCSD	CCSD(T)	DHF	CCSD	CCSD(T)
v2z	8.6285	9.2641	9.3863	-0.6261	-0.5162	-0.3209
v3z	8.6209	9.4117	9.5673	-0.3763	0.5705	0.8342
cv3z	8.6209	9.3748	9.5495	-0.3763	0.5304	0.8176
ae3z	8.6209	9.3603	9.5404	-0.3763	0.5151	0.8085
s-aug-v3z	8.6211	9.4123	9.5683	-0.3153	0.6411	0.9162
v4z	8.6209	9.4932	9.6696	-0.3329	0.6679	0.9597
cv4z	8.6209	9.4885	9.6724	-0.3329	0.6602	0.9612
ae4z	8.6209	9.4699	9.6607	-0.3329	0.6406	0.9494
s-aug-v4z	8.6209	9.4934	9.6699	-0.3152	0.6885	0.9852
d-aug-v4z	8.6209	9.4935	9.6699	-0.3150	0.6889	0.9857
t-aug-v4z	8.6209	9.4934	9.6699	-0.3150	0.6889	0.9857
s-aug-ae4z	8.6209	9.4702	9.6611	-0.3152	0.6616	0.9754
d-aug-ae4z	8.6209	9.4702	9.6611	-0.3150	0.6621	0.9761
d-aug-ae$N$z	8.6212	9.5498	**9.7479**	-0.3151	0.7143	**1.0338**

Table 7 summarizes the IP and EA results for Ds, for which the effects of using DHF, CCSD and CCSD(T) methods with a basis set can be compared. As for Pt, a clear trend is observed when comparing the computational methods. The addition of correlation treatment from DHF to CCSD has the largest effect on the IP and the EA, raising their values with about one eV. Contrary to the results for Pt, the EA of Ds is observed to be negative for the DHF method. This is because for Ds, an electron is added to the destabilized $6d_{5/2}$ orbital, which, without considering electron correlation, raises the total energy of the system. whereas for Pt, the electron is added to the stabilized and open 6s orbital, closing that orbital and lowering the total energy of the system.
The addition of perturbative triples further raises the IP and EA, but with a smaller amount of 0.2-0.3 eV. The EA is most sensitive to the computational method used, as the differences between its DHF, CCSD and CCSD(T) calculations are the largest.

Focusing on CCSD(T) results, the effects of basis sets will be evaluated.

Table 8: CCSD(T) results for split valence basis sets with increasing cardinalities.

CCSD(T)	IP	EA
v2z	9.3863	-0.3209
v3z	9.5673	0.8342
v4z	9.6696	0.9597

With Table 8, the effect of increasing the cardinality of a basis set can be assessed for Ds. Increasing from double to triple cardinality yields the largest increase in the IP and EA: 0.18 eV and 1.16 eV respectively. Further increasing to quadrupole cardinality increases both the IP and EA with 0.10 eV and 0.13 eV respectively. As for the computational method, increasing the basis set cardinality has a larger effect on the EA then on the IP.

Table 9: CCSD(T) results for the v4z basis set with outer-core correlating functions and inner-core correlating functions.

CCSD(T)	IP	EA
v4z	9.6696	0.9597
cv4z	9.6724	0.9612
ae4z	9.6607	0.9494

The effects of including outer-core correlating functions and inner-core correlating functions to the v4z split-valence basis set can be evaluated with Table 9. These effects are substantially smaller then those observed for the different cardinalities in Table 8. The addition of outer-core correlated functions increases the IP and EA with 2.8 and 1.5 meV's, respectively. Adding inner-core correlating functions and correlating all electrons leads to a negative correction for both the IP and EA with respect to both the v4z and cv4z basis sets. This effect is of an order larger then that of adding outer-core correlated functions, indicating that these inner-core orbitals participate more heavily in electron correlation.

Table 10: CCSD(T) results for the v4z basis set with the addition of single, double and triple diffuse functions.

CCSD(T)	IP	EA
v4z	9.6696	0.9597
s-aug-v4z	9.6699	0.9852
d-aug-v4z	9.6699	0.9857
t-aug-v4z	9.6699	0.9857

With Table 10, the addition of diffuse functions can be assessed for the IP and EA of Ds. The IP is barely affected: addition of a single layer of diffuse functions results in an increase of 0.3 meV and additional diffuse layers do not change the IP further. As expected, the EA is again affected more by the addition of diffuse functions as it benefits more from an qualitative description of the region far from the nucleus. The EA increases with 25.5 meV with the addition of a single layer of diffuse functions, and a small correction of 0.5 meV is observed for the addition of a second layer of diffuse functions. Addition of a third layer of diffuse functions does not further alter the EA. With respect to the third decimal, the results have thus converged after the second

layer of diffuse functions.

Since the effects on the IP and EA associated with the addition of diffuse functions are mostly independent of cardinality, inner, and outer core correlating functions, the results from Table 10 can be used to predict that the results converge as well after the second layer of diffuse functions for the ae4z basis set. Therefore, the CBS limit was taken for the d-aug-ae$N$z basis sets. For the IP, this yielded a final rounded value of 9.748 eV. The CBS limit corrected the IP with +86.8 meV with respect to the IP with the d-aug-ae4z basis set. For the EA, taking the CBS limit yielded a final rounded value of 1.034 eV. The CBS limit corrected the EA with +57.7 meV with respect to the d-aug-ae4z basis set.
The error associated with taking the CBS limit is calculated according to the procedure of [47], for which half of the difference between the CBS result and the d-aug-ae4z result is taken. This yields an error of 43.40 meV for the IP and 28.85 meV for the EA.

Table 11: A comparison of the results obtained with the v4z basis set in a non-relativistic framework; with the exact two-component Hamiltonian and with the Dirac four component Hamiltonian.

	IP			EA		
	DHF	CCSD	CCSD(T)	DHF	CCSD	CCSD(T)
non-relativistic (c=10000)	12.0281	7.0512	7.2748	3.8275	5.1432	5.3010
relativistic X2C	8.6498	9.5183	9.6940	-0.3060	0.6899	0.9803
relativistic 4C	8.6209	9.4932	9.6696	-0.3329	0.6679	0.9597

In Table 11, the IP and EA obtained with a non-relativistic calculation are compared to those obtained with relativistic calculations for a v4z basis set. As for platinum, the valence s- and d-orbitals were treated together as being open in the non-relativistic calculations. This resulted in the electrons being 'spread' equally over the orbitals, with 1/6th of the density on the 7s orbital and 5/6th of the density on the 6d orbitals for both the atom, the ion and the anion configurations.
In the relativistic frame, for the IP and the EA respectively, the electron is removed from or added to the relativistically destabilized $6d_{5/2}$ orbital. Therefore, the IP and the EA are expected to be lower there then in the non-relativistic frame, where an electron is removed from or added to both the 6d and 7s orbitals partially. These orbitals are both lower in energy then the relativistic $6d_{5/2}$ orbital, favoring the addition of an electron while disfavoring the removal of an electron there. This reasoning is followed by all calculations of the EA and by the DHF calculation of the IP. The CCSD and CCSD(T) calculations of the IP deviate from this logic, indicating that the effects of electron correlation overrule the expected effects for the IP. Overall, the large differences between the results obtained with non-relativistic and relativistic calculations again highlight the magnitude of treating relativity in heavy atom calculations. The importance of treating relativity is further underlined by the fact that the non-relativistic EA values are higher than any EA found in the periodic table, rendering them as very unrealistic [48].

Another comparison that can be made concerns the results obtained with the less computationally demanding X2C Hamiltonian and the results obtained with the Dirac 4C Hamiltonian. Here, a clear trend is observed where all values with the X2C Hamiltonian are 0.02-0.03 eV higher then those with the 4C Hamiltonian. The size of these differences underlines the quality of the approximation within the X2C Hamiltonian. While results were obtained much faster (15

minutes versus 1h and 14 minutes) with the X2C Hamiltonian and deviations with respect to the 4C Hamiltonian are less then 30 meV, accuracy within meV's is aimed for here. Therefore, in this research, the computational gain of the X2C Hamiltonian does not outweigh the accuracy of the 4C Hamiltonian.

5 Discussion

The calculated and rounded IP and EA for Darmstadtium with the CBS extrapolation on the d-aug-ae$N$z (N=2, 3, 4) basis sets and an orbital cut-off of -7000/2000 a.u. are 9.748 eV and 1.034 eV respectively. For Platinum, the calculated IP with the CBS limit on the d-aug-ae$N$z (N=2, 3, 4) basis sets and an orbital cut-off of -3000/2000 a.u. is 9.044 eV. The EA could not be calculated within the CBS limit due to the inaccuracy of the results obtained with triple cardinality basis sets. Therefore, the EA obtained with the d-aug-ae4z basis set was taken as the final value, being 2.192 eV.

Considering the general periodic trends outlined in section 2.2 for the IP and EA, the IP and EA of Ds were expected to be lower than those of Pt. Our results confirm that this is indeed the case for the EA, but that this expectation fails for the IP of Ds.

The electron affinity being lower for Ds than for its lighter homologue Pt can be explained by the differences in their electronic structures, combined with relativistic effects. For Ds, the anion is formed by the addition of an electron to the $6d_{5/2}$ orbital, which is expanded as a consequence of the relativistic s- and $p_{1/2}$-orbital contraction. The electrons in these contracted orbitals shield the outer orbitals from the nuclear charge, for which these outer orbitals experience a less strong pull towards the nucleus. This causes their radial expansion. Furthermore, the $6d_{5/2}$ orbital is raised in energy as a consequence of relativistic spin-orbit coupling. These relativistic effects make the addition of an extra electron in the $6d_{5/2}$ orbital less energetically favorable.
Whereas for Pt, the additional electron is added to the relativistically contracted and stabilized 6s orbital. Adding an electron here would close this stabilized orbital, which is energetically more favorable then the situation for Ds.

The same logic was expected to hold for the ionization potential. In Ds, an electron is removed from the destabilized and shielded $6d_{5/2}$ orbital whereas in Pt, an electron is removed from the stabilized 6s orbital. At first glance, this would imply a higher IP for Pt than for Ds, contrary to the outcome of our final calculations. Thus, there must be other effects that overrule these initial predictions. One possible explanation involves the ground state energies of both atoms. The ground state of Ds (-45057.7 a.u.) is about 2.44 times lower in energy than the ground state of Pt (-18437.0 a.u.). This implies that the electronic configuration of Ds is more stable than that of Pt, explaining why removing an electron from Ds would cost more energy as this would distort this stable configuration. This argument also complies with the lower EA of Ds.
Another possibility may involve relativistic screening effects. Although the valence d-orbitals are relativistically expanded and thus shielded from the nuclear charge by the inner electrons, other high angular momentum orbitals ($p_{3/2}$, d, f) are relativistically expanded as well, reducing their ability to screen the nuclear charge effectively. This relativistic effect is larger for Ds and may result in a higher effective nuclear charge felt for the Ds valence orbitals than for the Pt valence orbitals, increasing the IP for Ds. This argument however counteracts with the lower EA found for Ds. Further research on the electronic structure of Ds is needed to confirm any of the above arguments or to find new explanations.

When comparing the calculated IP and EA for Pt with the experimentally found IP and EA of 8.959 eV [15] and 2.125 eV [18] respectively, it we observe our results to respectively be +85 and

+67 meV higher than experiment. This suggests that the total effect of including higher order corrections would contribute a negative correction to the found values in the deV range.

For Ds, there exist no experimental IP or EA. An IP of 9.6 eV was reported in a review by Turler and Pershina [1] published in 2013. This review used the result from density functional theory calculations done in 1971 and 1975. In 2016, V.A. Dzuba reported an IP of 11.1567 eV for Ds, using relativistic Hartree-Fock and random-phase approximation methods [49]. This is significantly higher than any IP found with the CCSD(T) method for Ds. A master research project from 2018 reported an IP of 9.7386 eV using the DIRAC16 program for the CCSD(T) method with the CBS limit on a vNz basis set (N=2, 3, 4) and an orbital cut-off of -10000/300 a.u [50]. The paper reported an EA of 1.0147 eV with the same methods. These values are in accordance with our results in the deV range, and the smaller differences are explained considering that here a larger basis and a more recent version of DIRAC were used that raised the IP and EA. Finally, a recent bachelor thesis from 2022 reported an IP of 9,701 eV and an EA of 1,749 eV for Ds, using the DIRAC19 program for the CCSD(T) method with the CBS limit on a s-aug-vNz (N=2, 3, 4) basis set and no orbital cut-off [51]. The difference between their results and the current results may be explained by the larger basis set used in this paper, and by the more recent version of the Dirac program used. Furthermore, this 2022 thesis also experienced strange results with triple cardinality basis sets for the EA of platinum. This further confirms our hypothesis of the existence of some linear dependency within the triple zeta calculations involving the Pt anion.
Overall, when comparing our final results with those found in other theses using CCSD(T) method and CBS extrapolation, good accordance is found considering the differences in basis set and orbital cut-off.

The calculations in this thesis were performed using finite basis sets that were extrapolated to the complete basis set limit. The error associated with this is 43.4 meV for the IP and 28.85 meV for the EA of Ds. These basis set errors are expected to have the largest contribution to the total uncertainty of the calculations [26]. Furthermore, the active space used within our calculations was finite, and high energy virtual orbitals were cut off. When performing calculations with no orbital cut-off, a small correction may be imposed on the IP and EA. Moreover, the inability to specify the occupation of two open shells independently for the electronic configurations is another source of uncertainty for the DHF results. This is however less significant for coupled cluster calculations, as these require the specification of the occupation per m_j level. Other uncertainties may have arisen from the DIRAC23 program used, but these are expected to be small due to the narrow convergence criteria used within the calculations.

Besides uncertainties within the current methods used, there are higher order corrections missing from our calculations. First of all, electron correlation was not treated further then perturbative triples. In [50], the correction associated with the full triple contribution was found to be +1.042 eV for the IP of Ds. The correction from quadrupole excitations is expected to not exceed this tripe excitation contribution. Moreover, the calculated IP and EA are lacking higher order Breit and QED corrections. These corrections are expected to overrule the positive contribution from higher order excitations and thereby lower the IP and EA, considering the positive deviation of our Pt results with respect to experiment.

For future research on this topic and to improve the current accuracy of the results, higher order excitations should be included and Breit and QED corrections should be applied. More-

over, using the most recent version of DIRAC while increasing the active space of the coupled cluster calculations is encouraged.

6 Conclusion

The final rounded ionization potential and electron affinity of darmstadtium were calculated to be 9.748 eV and 1.034 eV respectively, using the CCSD(T) method with the Dirac Coulomb Hamiltonian. These calculations were obtained by performing the complete basis set extrapolation on the d-aug-ae$N$z basis, with N= 2, 3 and 4. The errors associated with the CBS limit are 42.40 and 28.85 meV for the IP and EA of Ds. The same computational methods yielded a final IP of 9.044 eV for platinum, with an associated CBS limit error of 0.95 meV. The final EA for platinum was found with the d-aug-ae4z basis set, yielding a value of 2.192 eV.
The calculated results for platinum are deV's higher than the experimentally established results, suggesting that higher order corrections will impose a negative correction within the deV range on the IP and EA for Pt and Ds. Corrections that are lacking are excitations of higher order than perturbative triples, the Breit correction and QED corrections. The implication of these corrections form a future prospect when research on this topic is to be continued.
The EA of Ds being lower than that of Pt agrees with expectations obtained from periodic trends and relativistic effects. The IP of Ds being higher than that of Pt disagrees with these expectations, and future research is needed to confirm the cause of this.
Treating relativity within the calculations was found to make a significant difference of a few eV's to the IP and EA of both Pt and Ds, highlighting its importance in heavy atom calculations. Apart from providing good and fast approximations, the X2C Hamiltonian was found to not be accurate enough to provide the aimed accuracy of meV's used in this thesis.

7 Bibliography

[1] A. Turler and V. Pershina, "Advances in the production and chemistry of the heaviest elements," *Chemical reviews*, vol. 113, 2013. [Online]. Available: https://doi.org/10.1021/cr3002438

[2] K. Bourzac, "Heaviest element yet within reach after major breakthrough," *Nature*, vol. 632, pp. 16–17, 2024. [Online]. Available: https://www-nature-com.proxy-ub.rug.nl/articles/d41586-024-02416-3

[3] S. A. Giuliani, Z. Matheson, W. Nazarewicz, E. Olsen, P.-G. Reinhard, J. Sadhukhan, B. Schuetrumpf, N. Schunck, and P. Schwerdtfeger, "Colloquium: Superheavy elements: Oganesson and beyond," *Rev. Mod. Phys.*, vol. 91, p. 011001, Jan 2019. [Online]. Available: https://link.aps.org/doi/10.1103/RevModPhys.91.011001

[4] P. Pyykko and J.-P. Desclaux, "Relativity and the periodic system of elements," *American Chemical Society*, vol. 12, 1979. [Online]. Available: https://doi.org/10.1021/ar50140a002

[5] S. Pappas, "Superheavies," *Scientific American Magazine*, vol. 330, p. 54, 2024. [Online]. Available: https://www-scientificamerican-com.proxy-ub.rug.nl/article/superheavy-elements-are-breaking-the-periodic-table/

[6] E. M. Holmbeck, J. Barnes, K. A. Lund, T. M. Sprouse, G. C. McLaughlin, and M. R. Mumpower, "Superheavy elements in kilonovae," *The Astrophysical Journal Letters*, vol. 951, no. 1, 2023. [Online]. Available: https://iopscience-iop-org.proxy-ub.rug.nl/article/10.3847/2041-8213/acd9cb/meta

[7] P. Patel, "Scientists find evidence of extremely heavy elements in ancient stars," 2023. [Online]. Available: https://cen.acs.org/physical-chemistry/astrochemistry/Scientists-find-evidence-extremely-heavy-elements-in-ancient-stars/101/web/2023/12

[8] V. Gupta, *Principles and applications of quantum chemistry*. Academic Press, 2015.

[9] J. P. Lowe and K. Peterson, *Quantum chemistry*. Elsevier, 2011.

[10] N. C. for Biotechnology Information, "Pubchem element summary for atomicnumber 110, darmstadtium," 2024. [Online]. Available: https://pubchem.ncbi.nlm.nih.gov/element/Darmstadtium

[11] C. Learner, "Darmstadtium." [Online]. Available: https://www.chemistrylearner.com/darmstadtium.html

[12] S. Hofmann, V. Ninov, F. P. Heßberger, P. Armbruster, H. Folger, G. Münzenberg, H. J. Schött, A. G. Popeko, A. V. Yeremin, A. N. Andreyev, S. Saro, R. Janik, and M. Leino, "Production and decay of^{269}110," *Zeitschrift fur Physik A Hadrons and Nuclei*, vol. 350, no. 4, pp. 277–280, December 1995. [Online]. Available: https://doi-org.proxy-ub.rug.nl/10.1007/BF01291181

[13] C. E. Düllmann, M. Block, and M. Manomivibul, "Island of heavy weights," *Scientific American*, vol. 318, no. 3, pp. pp. 46–53, 2018. [Online]. Available: https://www.jstor.org/stable/27173391

[14] H. Arbely, "High accuracy calculations of atomic properties of group v and group x elements," 2018. [Online]. Available: https://fse.studenttheses.ub.rug.nl/18206/1/FINAL.pdf

[15] N. I. of Standards and Technology, "Atomic data for platinum." [Online]. Available: https://physics.nist.gov/PhysRefData/Handbook/Tables/platinumtable1.htm

[16] J. d. P. Peter Atkins and J. Keeler, *Physical Chemistry*. Oxford University Press, 2018, ch. 8b.

[17] T. Moeller, J. C. Bailar, J. Kleinberg, C. O. Guss, M. E. Castellion, and C. Metz, "10 - periodic perspective: The representative elements," in *Chemistry*. Academic Press, 1980, pp. 273–298. [Online]. Available: https://www.sciencedirect.com/science/article/pii/B9780125033503500159

[18] T. Andersen, H. K. Haugen, and H. Hotop, "Binding energies in atomic negative ions: Iii," *J. Phys. Chem. Ref. Data*, vol. 28, 1999. [Online]. Available: https://doi-org.proxy-ub.rug.nl/10.1063/1.556047

[19] NIST, meet the constants. [Online]. Available: https://www.nist.gov/si-redefinition/meet-constants#:~:text=c%20is%20equal%20to%20299%2C792%2C458,the%20meter%2C%20kilogram%20and%20kelvin.

[20] T. A. Moore, *Six ideas that shaped physics*, 3rd ed. McGraw Hill, 2016, ch. Unit R.

[21] A. Das, U. Das, R. Das, and A. K. Das, "Relativistic effects on the chemistry of heavier elements: why not given proper importance in chemistry education at the undergraduate and postgraduate level?" *Chemistry Teacher International*, vol. 5, no. 4, pp. 365–378, 2023. [Online]. Available: https://doi.org/10.1515/cti-2023-0043

[22] J. C. Morrison, *Modern Physics for Scientists and Engineers*, 2nd ed. Elsevier, 2015, ch. 4: The Hydrogen atom.

[23] C. D. Sherrill, *An Introduction to Hartree-Fock Molecular Orbital Theory*. Georgia Institute of Technology; School of Chemistry and Biochemistry, 2000.

[24] A. Borschevsky. (2023) Lectures materials design. [Online]. Available: https://brightspace.rug.nl/d2l/common/dialogs/quickLink/quickLink.d2l?ou=356427&type=lti&rcode=8AE7AF6F-0534-48B3-97C6-4FDC1563223B-63518&srcou=6606&launchFramed=1&framedName=Kaltura+Videos+%26+Classroom

[25] J. Toulouse, *Introduction to perturbation theory and coupled-cluster theory for electron correlation*. Université Pierre et Marie Curie, 2017.

[26] Y. G. et al, "Relativistic coupled cluster calculations of the electron affinity and ionization potential of nh(113)," *Journal of Physics B: Atomic, Molecular and Optical Physics*, vol. 55, 2022. [Online]. Available: https://iopscience-iop-org.proxy-ub.rug.nl/article/10.1088/1361-6455/ac761f/meta

[27] Reed College, "Relativistic quantum mechanics ii: lecture 35." [Online]. Available: https://www.reed.edu/physics/courses/Physics342/html/page2/files/Lecture.35.pdf

[28] J. Heully, I. Lindgren, E. Lindroth, S. Lundqvist, and A. M. Martensson-Pendrill, "Diagonalisation of the dirac hamiltonian as a basis for a relativistic many-body procedure," *Journal of Physics B: Atomic and Molecular Physics*, vol. 19, no. 18, p. 2799, sep 1986. [Online]. Available: https://dx.doi.org/10.1088/0022-3700/19/18/011

[29] R. F. Bishop and H. G. Kummel, "The coupled-cluster method," *Physics Today*, 1987. [Online]. Available: https://doi-org.proxy-ub.rug.nl/10.1063/1.881103

[30] I. Y. Zhang and A. Grüneis, "Coupled cluster theory in materials science," *Frontiers in Materials*, vol. 6, 2019. [Online]. Available: https://www.frontiersin.org/journals/materials/articles/10.3389/fmats.2019.00123

[31] R. J. Bartlett and M. Musiał, "Coupled-cluster theory in quantum chemistry," *Rev. Mod. Phys.*, vol. 79, pp. 291–352, Feb 2007. [Online]. Available: https://link.aps.org/doi/10.1103/RevModPhys.79.291

[32] K. Lipkowitz and D. Boyd, *Reviews in Computational Chemistry, Volume 14*, ser. Reviews in Computational Chemistry. Wiley, 2009. [Online]. Available: https://books.google.nl/books?id=HKUqzEV7to4C

[33] G. E. Scuseria and T. J. Lee, "Comparison of coupled-cluster methods which include the effects of connected triple excitations," *The Journal of Chemical Physics*, vol. 93, no. 8, pp. 5851–5855, 1990. [Online]. Available: https://doi.org/10.1063/1.459684

[34] J. F. Stanton, "Why ccsd(t) works: a different perspective," *Chemical Physics Letters*, vol. 281, no. 1, pp. 130–134, 1997. [Online]. Available: https://www.sciencedirect.com/science/article/pii/S0009261497011445

[35] T. Saue, "Relativistic Hamiltonians for Chemistry : A Primer," *ChemPhysChem*, vol. 12, no. 17, pp. 3077–3094, Dec 2011. [Online]. Available: https://hal.science/hal-00662643

[36] M. Iliaš and T. Saue, "An infinite-order two-component relativistic Hamiltonian by a simple one-step transformation," *The Journal of Chemical Physics*, vol. 126, no. 6, 02 2007. [Online]. Available: https://doi.org/10.1063/1.2436882

[37] C. Tantardini, R. D. R. Eikås, M. Bjørgve, S. R. Jensen, and L. Frediani, "Full breit hamiltonian in the multiwavelets framework," *Journal of Chemical Theory and Computation*, vol. 20, 2024. [Online]. Available: https://doi-org.proxy-ub.rug.nl/10.1021/acs.jctc.3c01056

[38] Y. Guo, L. c. v. F. Pašteka, Y. Nagame, T. K. Sato, E. Eliav, M. L. Reitsma, and A. Borschevsky, "Relativistic coupled-cluster calculations of the electron affinity and ionization potentials of lawrencium," *Phys. Rev. A*, vol. 110, p. 022817, Aug 2024. [Online]. Available: https://link.aps.org/doi/10.1103/PhysRevA.110.022817

[39] P. Atkins and R. Friedman, *Molecular Quantum Mechanics*, 5th ed. Oxford University Press, 2011, ch. 9. [Online]. Available: http://www.nanoer.net/d/img/Molecular%20Quantum%20Mechanics,%205th%20Edition.pdf

[40] B. Nagy and F. Jensen, *Basis Sets in Quantum Chemistry*. John Wiley Sons, Ltd, 2017, ch. 3, pp. 93–149. [Online]. Available: https://onlinelibrary.wiley.com/doi/abs/10.1002/9781119356059.ch3

[41] Diracprogram.org, "Pick the right basis for your calculation." [Online]. Available: https://www.diracprogram.org/doc/release-13/molecule_and_basis/basis.html

[42] V. Vasilyev, "Online complete basis set limit extrapolation calculator," *Computational and Theoretical Chemistry*, vol. 1115, pp. 1–3, 2017. [Online]. Available: https://www.sciencedirect.com/science/article/pii/S2210271X17302888

[43] DIRAC, a relativistic ab initio electronic structure program, Release DIRAC23 (2023), written by R. Bast, A. S. P. Gomes, T. Saue and L. Visscher and H. J. Aa. Jensen, with contributions from I. A. Aucar, V. Bakken, C. Chibueze, J. Creutzberg, K. G. Dyall, S. Dubillard, U. Ekström, E. Eliav, T. Enevoldsen, E. Faßhauer, T. Fleig, O. Fossgaard, L. Halbert, E. D. Hedegård, T. Helgaker, B. Helmich–Paris, J. Henriksson, M. van Horn, M. Iliaš, Ch. R. Jacob, S. Knecht, S. Komorovský, O. Kullie, J. K. Lærdahl, C. V. Larsen, Y. S. Lee, N. H. List, H. S. Nataraj, M. K. Nayak, P. Norman, A. Nyvang, G. Olejniczak, J. Olsen, J. M. H. Olsen, A. Papadopoulos, Y. C. Park, J. K. Pedersen, M. Pernpointner, J. V. Pototschnig, R. di Remigio, M. Repisky, K. Ruud, P. Sałek, B. Schimmelpfennig, B. Senjean, A. Shee, J. Sikkema, A. Sunaga, A. J. Thorvaldsen, J. Thyssen, J. van Stralen, M. L. Vidal, S. Villaume, O. Visser, T. Winther, S. Yamamoto and X. Yuan (available at https://doi.org/10.5281/zenodo.7670749, see also https://www.diracprogram.org).

[44] Hábrók HPC cluster of the University of Groningen. [Online]. Available: https://wiki.hpc.rug.nl/habrok/start

[45] MobaXterm: Enhanced terminal for Windows with X11 server, tabbed SSH client, network tools and much more. [Online]. Available: https://mobaxterm.mobatek.net/

[46] NIST, "The nist reference on constants, units and uncertainty; fundamental physical contanst," 2022. [Online]. Available: https://physics.nist.gov/cgi-bin/cuu/Value?hrev

[47] K. J. G. Y. e. a. Leimbach, D., "The electron affinity of astatine," *Nat Commun*, vol. 11, 2020. [Online]. Available: https://doi.org/10.1038/s41467-020-17599-2

[48] N. L. of Medicine, "Periodic table of elements." [Online]. Available: https://pubchem.ncbi.nlm.nih.gov/periodic-table/#property=ElectronAffinity

[49] V. A. Dzuba, "Ionization potentials and polarizabilities of superheavy elements from db to cn ($z = 105 - -112$)," *Phys. Rev. A*, vol. 93, p. 032519, Mar 2016. [Online]. Available: https://link.aps.org/doi/10.1103/PhysRevA.93.032519

[50] H. Arbely, "High accuracy calculations of atomic properties of group v and group x elements," Master's thesis, University of Groningen, 2018. [Online]. Available: https://fse.studenttheses.ub.rug.nl/18206/1/FINAL.pdf

[51] M. Veld, "Ionization potential and electron affinity of darmstadtium," University of Groningen, Tech. Rep., 2022. [Online]. Available: https://fse.studenttheses.ub.rug.nl/28371/1/bPHYS_2022_VeldM.pdf